AD-A168 133 REAL TIME MATH MODEL FOR INFRARED(U) GEORGIA INST OF 1/1
TECH ATLANTA SCHOOL OF ELECTRICAL ENGINEERING
D R HERTLING ET AL. JAN 86 GIT/E4857A-85 RADC-TR-85-247
UNCLASSIFIED F30602-81-C-0185 F/G 17/5 NL

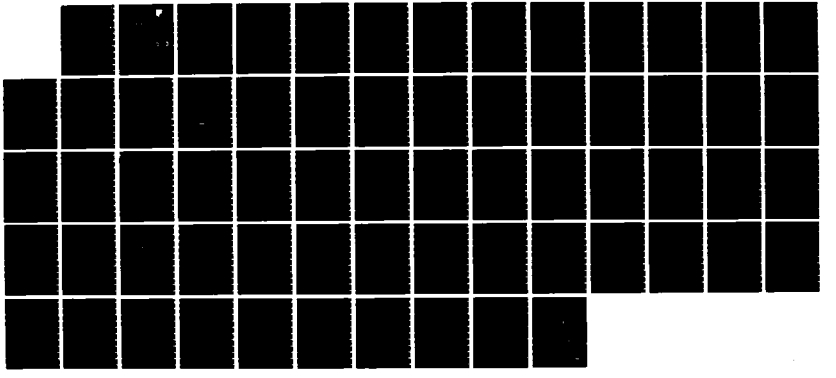

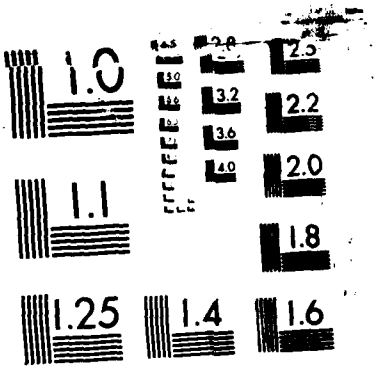

MICROCOPY RESOLUTION TEST CHART

RADC-TR-85-247
Final Technical Report
January 1986

REAL TIME MATH MODEL FOR INFRARED

Georgia Institute of Technology

David R. Hertling and R. C. Rearick

This effort was funded totally by the Laboratory Directors' Fund

ROME AIR DEVELOPMENT CENTER
Air Force Systems Command
Griffiss Air Force Base, NY 13441-5700

This report has been reviewed by the RADC Public Affairs Office (PA) and is releasable to the National Technical Information Service (NTIS). At NTIS it will be releasable to the general public, including foreign nations.

RADC-TR-85-247 has been reviewed and is approved for publication.

APPROVED: John B. Sterling, III

JOHN B. STERLING, III
Project Engineer

APPROVED: Walter J. Senus

WALTER J. SENUS
Technical Director
Intelligence & Reconnaissance Division

FOR THE COMMANDER: Richard W. Pouliot

RICHARD W. POULIOT
Plans & Programs Division

If your address has changed or if you wish to be removed from the RADC mailing list, or if the addressee is no longer employed by your organization, please notify RADC (IRRP) Griffiss AFB NY 13441-5700. This will assist us in maintaining a current mailing list.

Do not return copies of this report unless contractual obligations or notices on a specific document requires that it be returned.

REPORT DOCUMENTATION PAGE

1a REPORT SECURITY CLASSIFICATION UNCLASSIFIED	1b RESTRICTIVE MARKINGS N/A
2a SECURITY CLASSIFICATION AUTHORITY N/A	3 DISTRIBUTION / AVAILABILITY OF REPORT Approved for public release; distribution unlimited.
2b DECLASSIFICATION / DOWNGRADING SCHEDULE N/A	
4 PERFORMING ORGANIZATION REPORT NUMBER(S) 4857A-85	5 MONITORING ORGANIZATION REPORT NUMBER(S) RADC-TR-85-247
6a NAME OF PERFORMING ORGANIZATION Georgia Institute of Technology 6b OFFICE SYMBOL (If applicable)	7a NAME OF MONITORING ORGANIZATION Rome Air Development Center (IRRP)
6c ADDRESS (City, State, and ZIP Code) School of Electrical Engineering Atlanta GA 30332	7b ADDRESS (City, State, and ZIP Code) Griffiss AFB NY 13441-5700
8a NAME OF FUNDING / SPONSORING ORGANIZATION Rome Air Development Center 8b OFFICE SYMBOL (If applicable) IRRP	9 PROCUREMENT INSTRUMENT IDENTIFICATION NUMBER F30602-81-C-0185
8c ADDRESS (City, State, and ZIP Code) Griffiss AFB NY 13441-5700	10 SOURCE OF FUNDING NUMBERS PROGRAM ELEMENT NO: 61101F; PROJECT NO: LDFP; TASK NO: 05; WORK UNIT ACCESSION NO: P2

11 TITLE (Include Security Classification)
REAL TIME MATH MODEL FOR INFRARED

12 PERSONAL AUTHOR(S)
David R. Hertling, R. C. Rearick

13a TYPE OF REPORT	13b TIME COVERED	14 DATE OF REPORT (Year, Month, Day)	15 PAGE COUNT
Final	FROM Jun83 TO Sep85	January 1986	64

16 SUPPLEMENTARY NOTATION
This effort was funded totally by the Laboratory Directors' Fund.

17 COSATI CODES			18 SUBJECT TERMS (Continue on reverse if necessary and identify by block number)
FIELD	GROUP	SUB-GROUP	
08	02		Math Model; Signal Processing; Infrared Imagery; Photogrammetry
09	02		

19 ABSTRACT (Continue on reverse if necessary and identify by block number)

The main objective of this work was to access the feasibility of developing a real time math model which could be used to process infrared imagery with current real-time stereo compilation equipment. A survey of existing infrared sensors, imaging sensors, photogrammetric techniques and procedures for stereo viewing and plotting are presented. A flexible system model was developed which can be adapted to various types of infrared imaging systems.

Investigations revealed that the photogrammetric techniques accurate enough for mapping and targeting applications require accurate flight dynamics data which must be simultaneously recorded with the imagery. It is theoretically possible to process certain images which contain known or analytically solvable ground information; however, such procedures would depend upon the image itself and would not be amenable to evolving into a generalized math model.

20 DISTRIBUTION / AVAILABILITY OF ABSTRACT	21 ABSTRACT SECURITY CLASSIFICATION
☒ UNCLASSIFIED/UNLIMITED ☐ SAME AS RPT ☐ DTIC USERS	UNCLASSIFIED
22a NAME OF RESPONSIBLE INDIVIDUAL John B. Sterling, III	22b TELEPHONE (Include Area Code) (315) 330-4379
	22c OFFICE SYMBOL RADC (IRRP)

DD FORM 1473, 84 MAR 83 APR edition may be used until exhausted
All other editions are obsolete

Simultaneous recording of infrared and visible imagery along with accurate flight dynamics data in a digital format is recommended. This would allow maximum utilization of current and future photogrammetric, computer graphics and digital signal processing techniques.

17. COSATI CODES (Continued)

Field	Group
15	04

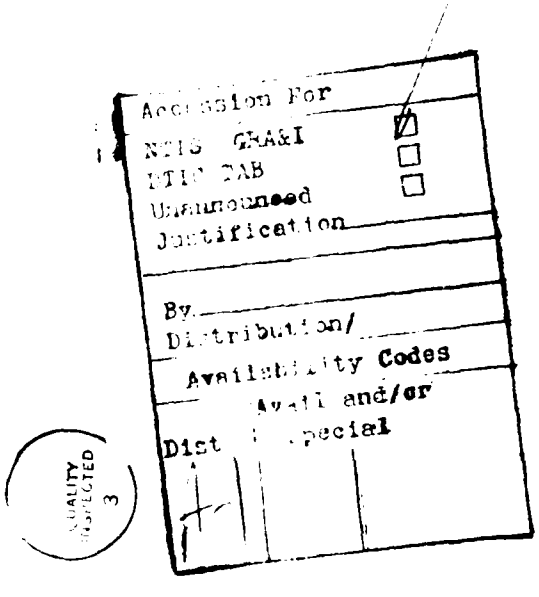

TABLE OF CONTENTS

		PAGE
	LIST OF ILLUSTRATIONS	iii
1.0	INTRODUCTION	1
2.0	INFRARED IMAGING	2
	2.1 Comparison of Visible and IR Imagery	2
	2.1 Detector Unit Cells	3
	2.2.1 CCD Unit Cells	4
	2.2.2 CID Unit Cells	6
	2.3 Operational Array Modes	11
	2.3.1 Staring Arrays	11
	2.3.2 Scanned Arrays	13
	2.4 Construction of Focal Plane Arrays	14
	2.5 Practical Consideration	17
3.0	PHOTOGRAMMETRIC CONSIDERATIONS	19
	3.1 Strip Cameras	20
	3.2 Linear TDI Arrays	20
	3.3 Processing of Strip Photography Data	23
	3.3.1 Line-by-Line Orientation	24
	3.3.2 Section-by-Section Orientation	26
	3.3.3 Triple Channel Recording	28
	3.3.4 Processing Stereo Line Image Data	30

4.0 RESOLUTION MODEL 34

4.1 Resolution of Solid State Imagers 36

4.2 System Model 44

4.3 Application of the System Model 46

5.0 CONCLUSIONS AND RECOMMENDATIONS 48

APPENDIX REAL TIME RESPONSE 50

REFERENCES 53

LIST OF ILLUSTRATIONS

FIGURE		PAGE
1	CCD Unit Cell	5
2	Readout of CCD Unit Cells	7
3	CID Unit Cell	8
4	Readout of CID Unit Cells	10
5	Staring Array	12
6	Scanned Array	15
7	Linear TDI Array	21
8	Storage of line data for line-to-line orientation	25
9	a. Storage of section data for section-to-section orientation	27
	b. Coordinate system	27
10	Storage of data for triple channel recording	29
11	Push-broom scanned array	35
12	Linear array with staggered detectors	38
13	a. Quantum energy integrated by detector elements from a single point spread distribution	40
	b. Two points resolved at the Nyquist rate	40
	c. Two points unresolved	40
14	Point spread model function	43

1.0 Introduction

The main objective of this project is to assess the feasibility of developing a mathematical model for IR imaging sensors which could be used in real-time stereo compilation equipment and tactical Air Force targeting applications. The work was divided as follows.

1. A survey of existing IR sensors and imaging systems.
2. A survey of photogrammetric techniques and procedures for stereo viewing and plotting.
3. Development of a flexible system model which can be adapted to various types of IR imaging systems.

During this work, particular attention was paid to integrating IR imagery into existing equipment and procedures. Recommendations are also made with regard to future systems which will be able to capitalize on emerging computer graphics technologies.

The organization of the report is as follows. Section 2 gives a brief overview of IR imaging and the available types of IR detectors and focal plane arrays. This overview has been limited to the technologies most likely to be used for modern IR imaging systems. Section 3 discusses photogrammetric considerations and furthermore concentrates on those most pertinent to the needs of Air Force and DMA. Section 4 introduces and describes the system model which was developed and is adaptable to any one of the candidate imaging systems. Finally, Section 5 presents the conclusions of this work and discusses various alternatives in integrating IR imagery into existing operations.

2.0 Infrared Imaging

There are several kinds of IR imaging systems. This section briefly describes various IR imaging systems and concentrates and those most likely to be used for aerial imagery collection.

2.1 Comparison Between IR and Visible Imagery

Conventional visible photography is a very mature technology. Over the years, improvements in photographic emulsions have yielded films which are capable of very high resolution. Visible photography lies roughly in the .4 to .7 micron region of the electromagnetic spectrum. Typically, aerial photographic systems filter out light toward the blue end of the spectrum.

Photographic films are available which are sensitive into the near infrared (.7 to .9 micron). These films are used to image IR radiation reflected from objects as opposed to IR radiation radiated from objects. Usually the source of IR radiation is the sun, however, for some applications an artifical IR source is used to illuminate the scene.

The primary reason IR photography and electronic imagery lag their visible counterparts is the lack of photoconductive and photoemissive materials which operate at IR wavelengths. Both photoconductivity and photoemissivity are quantum processes which depend upon the absorption of photons. Photons with wavelengths greater than approximately 1

micron simply do not have sufficient energy to be absorbed by most photoconductive and photoemmissive materials. There are some exotic materials which work further out into the infrared, however, they have other limitations such as the need to be cooled and low sensitivity. In recent years, significant advances in electronic IR imaging devices have been made. The most popular of these are Charge-Coupled-Device (CCD) and Charge-Injection-Device (CID) unit cell focal plane arrays. Linear or rectangular arrays of these unit cells are often operated in a time-delay-and-integrate (TDI) mode in order to increase the sensitivity of the array. In this mode both the scene and its corresponding electrical analog move along the array in a "pushbroom" fashion. This type of operation actually forms an electronic equivalent of a strip camera. A brief description of strip cameras will be given in a later section.

2.2 Detector Cells

The unit detector cell is the most elementary part of the detector array. The unit cell which is chosen governs the application for which the array shall be used in addition to determining the overall performance and operation of a particular array. The primary function of the unit cell is to convert IR radiation to a usable electrical form which then undergoes various stages of signal processing. Requirements for unit cell operation include: low noise, low circuit complexity, high uniformity of response, high injection efficiency, and high dynamic range [1]. The most popular types of unit cells are those

which employ charge coupling (CCD) and charge injection (CID). Neither device is better than the other, however, they each have their own advantages and disadvantages.

2.2.1 CCD Unit Cells

The CCD is probably the more popular of these two unit cells mainly due to its simplicity of operation and fabrication. The basic CCD unit cell is shown in Figure 1.

IR radiation strikes the detector portion of the unit cell, characterized by a photodiode, which is coupled into an integrating well. This well is basically a capacitor which stores accumulated charge. A transfer gate provides the path for current to flow from the photodiode to the well. A certain amount of time, called the integration time, is required to fill the well. Each well is then electronically scanned by a shift register which transfers the charge to the next CCD cell. Eventually the charge is transferred out of the array and the process can be repeated.

The charge capacity of the CCD is dependent upon several factors. The maximum charge storage possible is limited by the density of the array as this limits the size of the well. The maximum voltage which may be applied to the photodiode is limited by breakdown and tunneling considerations. In addition, overcharging of the well must be avoided otherwise an effect known as blooming can occur. Lastly, there is a strong temperature dependence for the charging mechanism. Typically

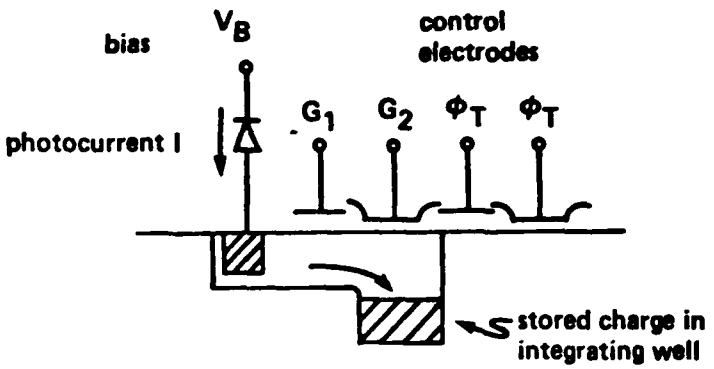

Figure 1. CCD Unit Cell [1].

these detectors are kept at a constant temperature (often 77°K) to limit the amount of dark current. Dark current flows when the photodiode is not illuminated and ideally no current is flowing. Performance of the CCD cells is also affected by the purity of materials used in the fabrication of the well and detector [2,3].

Another consideration for CCD operation is the accessibility of the electrical signals from each CCD cell. Figure 2 provides an illustration of two schemes. One possible way to transfer signals out is serially via a multiplexer. This method is used for applications where long intervals are required due to excessive signal processing. Another method interfaces in a parallel fashion and thus allows for shorter integration times. Since integration times are basically controlled by the clock rate of the shift registers, these rates may be varied electronically to provide variable sensitivity.

2.2.2 CID Unit Cells

The CID detector may be described as a surface channel device that employs intracell charge transfer and charge injection to achieve the solid state image sensing function [4]. A basic CID cell is shown in Figure 3. This cell basically consists of a detector, a metal-oxide semiconductor (MOS) capacitor, and gates. Photocurrent is generated when IR radiation falls on the detector which in turn charges the MOS capacitor. As the capacitor charges it is basically integrating. At some point in the charging period, a gate is closed connecting the

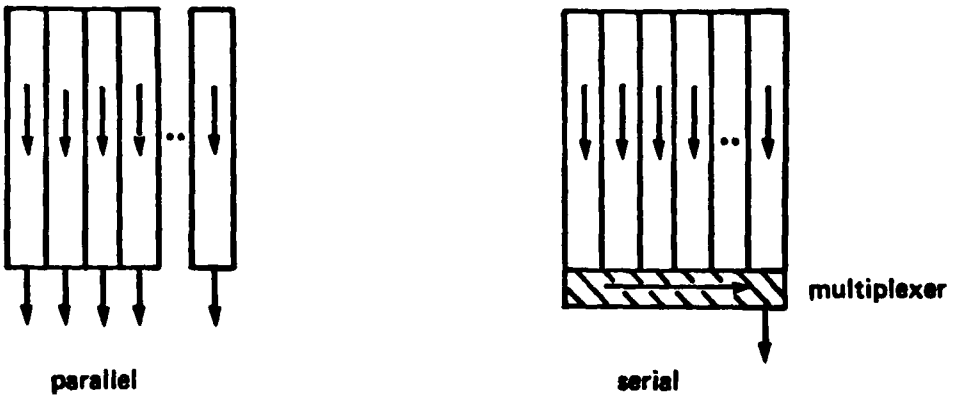

Figure 2. Readout of CCD Unit Cells [6].

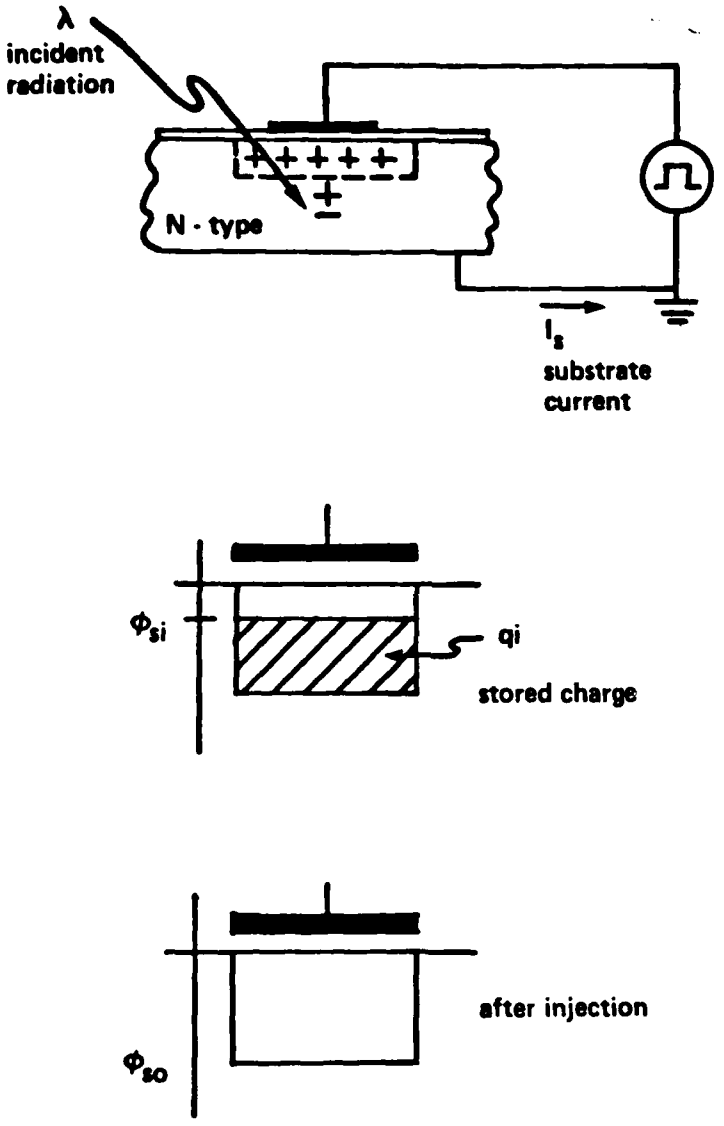

Figure 3. CID Unit Cell [4].

capacitor to the substrate, discharging charging and discharging is controlled by an electrical network as illustrated in Figure 4. This electrical network is called an x-y matrix which allows any cell to be addressed and thus read. There are various sensing schemes used which include sequential injection, preinjection, and parallel injection. Sequential injection scans the matrix by selecting a row and pulsing the sequential columns to read the row. Reading all rows sequentially results in a raster scan of the detector array. The preinjection technique relies on sensing a change in charge when a complete row is injected simultaneously. Each row is charged (preinjected) prior to sensing and then each detector cell discharges proportional to its photocurrent. The change in charge is measured when the charge of a detector is injected into the substrate. Parallel injection allows the function of charge detection to be separated from charge injection. The rows are selected and sensed in parallel allowing fast detection. The performance of CID arrays is dependent on several factors. First of all, temperature plays a large part in the production of dark current which directly effects the dynamic range. The maximum voltage is determined by the breakdown and tunneling of MOS devices used as gates. Lastly, high data rates and low signal levels of the cells require the use of processing amplifiers that are low in noise and high in bandwidth. This additional circuitry must be small in size and low in power consumption [5].

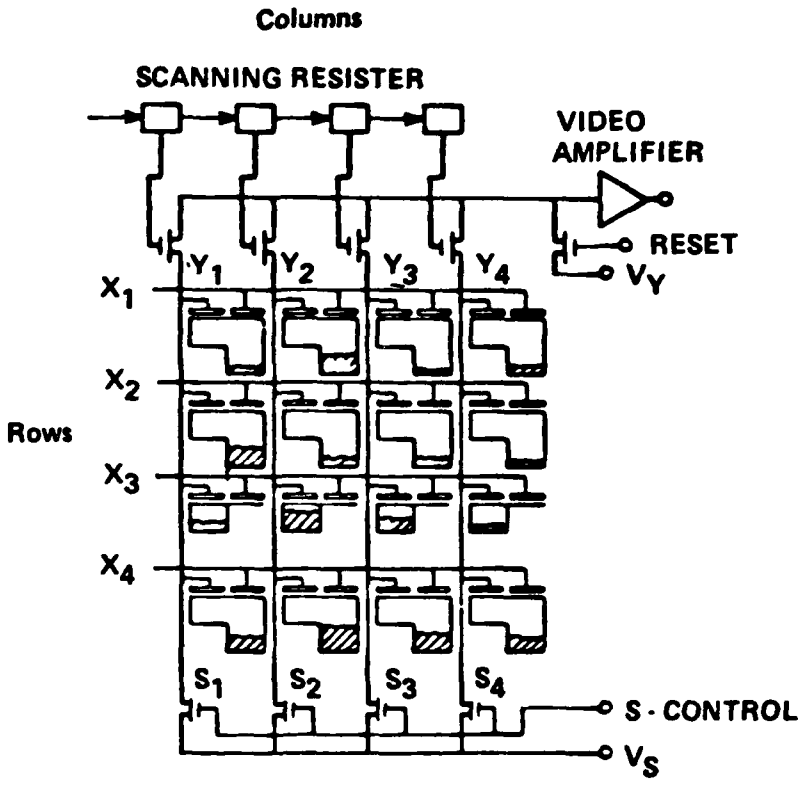

Figure 4. Readout of a matrix of CID unit cells [4].

2.3 Operational Array Modes

Depending upon system resolution, cost, and application, several operational array modes may be chosen. These modes may be divided into two basic groups, staring arrays and scanning arrays. The difference between these two modes is that staring arrays continuously "look" at the scene while scanning arrays are time gated.

2.3.1 Staring Arrays

Staring arrays can be constructed as either two-dimensional mosaic arrays or as one dimensional linear arrays. A typical staring array system is pictured in Figure 5. In this diagram, energy emitted from the scene is focused onto a two-dimensional mosaic array of IR detectors. The mosaic array is typically constructed from a large number of detectors arranged in a two dimensional pattern. One method of fabricating such an array is to butt several smaller arrays say, for example, 1024 x 64 together. This is often necessary because of the difficulty of constructing large mosaic arrays in one fabrication.

One disadvantage of staring arrays, however, is their lack of sensitivity. One commonly used way to increase the sensitivity is to operate detectors in a mode which allows the sensors to integrate signal over as long a time as possible. A method of achieving this integration of the signal is called Time-Delay-and-Integrate (TDI). There is a practical limit, however, on the length of integration time. The detectors basically accumulate charge during the integration time

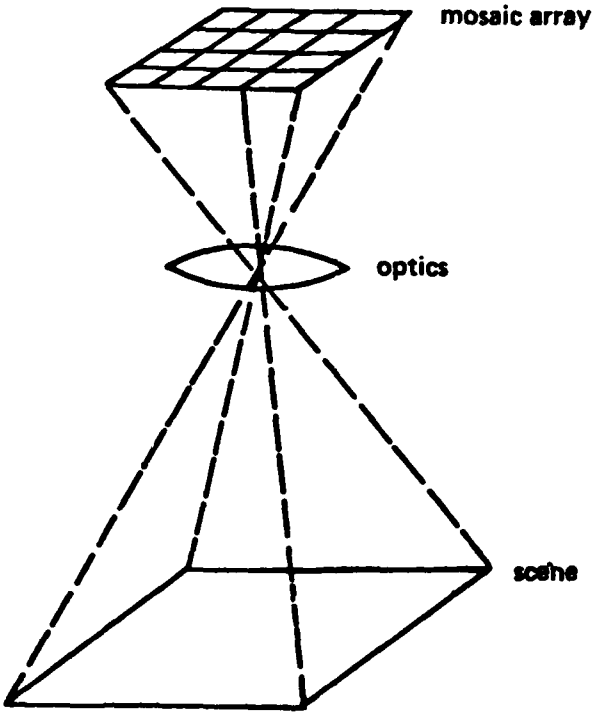

Figure 5. Staring Array.

and, since each detector element can hold so much charge, the amount of accumulated charge is limited.

There are other problems associated with mosaic staring arrays. Most of these problems originate from the single most critical part of the system, the mosaic array. Because a large number of detectors are used to make up a focal plane, non-uniformity of the responsivity of each detector may present a problem. In addition, the assembly of a large focal plane by butting smaller arrays can cause a loss of active elements along a butt seam resulting in lower resolution along seams. Lastly, when large integration times are used, large background levels can swamp out the smaller AC signal [2].

2.3.2 Scanned Arrays

An alternative to staring arrays is the scanned array [3-5]. Radiation emitted from the scene is reflected onto the detector array by a rotating mirror or prism. When the orientation of the mirror is such that it reflects the scene radiation normal to the detector array, the detectors are illuminated. By varying the speed of rotation of the mirror, the amount of radiation from the scene incident on the detector can be controlled. The scanning mirror, therefore, can provide the same function as the shutter in a camera. The orientation of the linear array with respect to the projected scene is vital. The linear array, which is rectangular in shape, is orientated such that the direction of motion of the array is perpendicular to the long side of

the array as illustrated in Figure 6. By having such an orientation, a rectangular strip image may be recorded every time the mirror projects radiation onto the array. The detector images may be electronically stored and assembled to form a single continuous image of width w and length nL where n is the number of rotations of the mirror.

2.4 Construction of Focal Plane Arrays

Depending upon cut-off wavelength, complexity, and cost, several construction and fabrication techniques may be chosen for the manufacture of focal plane arrays. There are basically two classes in which these arrays may be divided, monolithic and hybrid. In general, monolithic focal planes collect, transfer and store charge from IR radiation in a single medium. Hybrid focal planes, however, detect the IR radiation in a sensing medium which is electrically and mechanically connected to a different medium. The materials composing the detectors and IR semiconductors include PbTe, PbSnTe, InSb, InAsSb, InGaSb, PbS, PbSeTe, and HgCdTe [5].

Desirable properties of the focal plane array include: high uniformity of response, high flexibility for tests and diagnosis, and low dead space [1]. The first and third of these depend on mechanical design and construction of the array. Non-uniform response may also be caused by non-uniform temperature distributions or impurities in the substrate. Excessive dead space may be caused by the mechanical imprecision of chip butting which is necessary in the assembly of

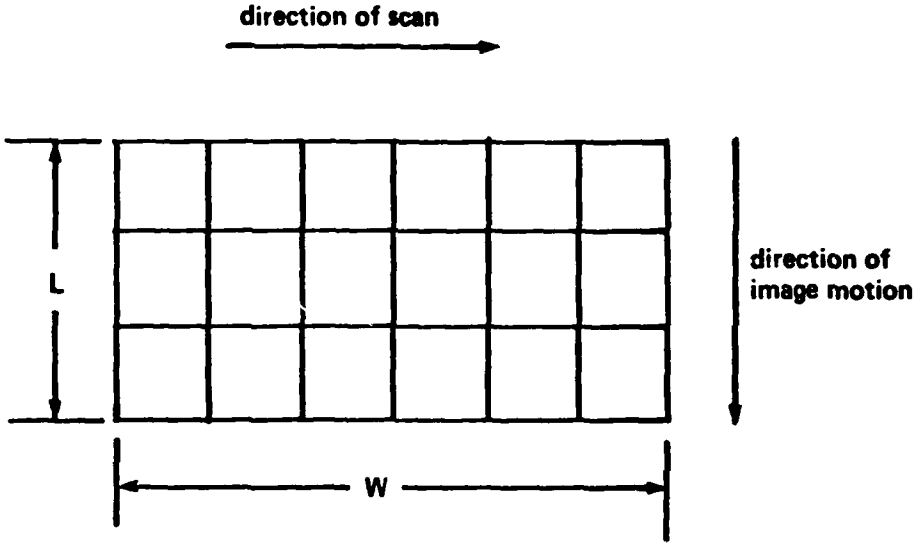

Figure 6. Scanned Array.

mosaic arrays. Testing and diagnosis may include a self test to determine whether each cell or array is operating properly. These tests are only possible with additional hardware and thus higher electronic complexity.

Depending on the materials used for the array and detector manufacture, different cut-off wavelengths are attainable. However, each of these materials has advantages and disadvantages which must be considered. As to actual manufacture of focal planes, the monolithic technology is probably the most limited. One limitation is in the detector region since each cell cannot be individually optimized. The reason for this lies in the fact that the optimization of one layer at an elevated temperature will lead to the degradation of the other [8]. This temperature problem is inherent since focal plane temperatures are often kept at 77 $^{\circ}$K. The main advantage of the monolithic technology, however, is its relatively low production cost due to its simplicity of construction.

The hybrid focal plane array may be described as an integrated multi-element array. Therefore, increased mechanical and thus higher construction complexity result. There are several methods which are used to mechanically mount the detectors. Examples of two common methods are direct and flip chip or solder bump mounting [5].

An additional consideration in array manufacture is electrical connection of detectors. In mosaic arrays particularly, there is usually some scheme for reading the individual detectors (e.g. serial

or parallel). Therefore, the necessary reading lines could contribute, to a large extent, to the complexity of each array.

2.5 Practical Considerations

In any system which is to be implemented, there are numerous practical factors to be considered [5-8]. These are often not directly obvious from theoretical discussions. In the design of IR imaging systems, design considerations focus mainly on the detector array. These considerations may be divided into three basic groups: mechanical, electrical, and optical.

Mechanical considerations include secure mounting of the array to the imaging system. Movement of the array due to external vibrations can cause loss of resolution as well as possible damage to the array. Any moving parts, such as rotating mirrors should be sufficiently rugged to withstand vibration and shocks associated with airborne vehicles. The array itself should also be rugged, especially in the case of mosaic arrays, so that mechanical and electrical connections do not fail. A further consideration may be the actual size and weight of the IR imaging system. Excessive size and weight would require possible modification of existing flight vehicles. Finally, there should be provisions for cryogenic systems to provide cooling for the detector arrays.

Electrical considerations, much like the mechanical considerations, depend on their physical surroundings. Ambient temperature may have an influence on precision electronics, particularly for high altitude flight.

Optical system requirements are very stringent since the transfer of IR information from the scene to the detector is a critical step in detection. The resolution of the system is limited by the detector spacing of the focal plane. The IR optical system must be designed so as not to degrade resolution. The design of IR optical systems is further complicated by the limited number of materials transparent to IR radiation.

3.0 Photogrammetric Considerations

The integration of IR imagery into Air Force and DMA operations involves two important considerations. These are;

1. How can this extra capability be most easily added with the least amount of modification to existing equipment and procedures?

2. In the absence of any constraints imposed by present equipment and procedures, what is the best method to integrate IR capability?

Stereocomparators and stereocompilers are computer controlled image measurement systems used for the processing of visible imagery. These systems are multi-stage stereocomparators which have been interfaced with digital computers and special display and control equipment. The addition of the computer and control equipment to a stereocomparator relieves the operator of many of the laborious and tedious tasks involved with the processing of imagery and thus greatly improves operator productivity. From a systems standpoint, the stereocomparator can be modeled as a system whose inputs are Reseau data and images stored on photographic media. The outputs of the system are point coordinates.

In order to consider adding IR imagery to the existing stereocomparator, one must consider how to input the IR data. It is assumed that the same output data will be desired for either IR or visible imagery.

3.1 Strip Cameras

A strip camera operates by moving film past a narrow slit which functions as an "open shutter". The speed of the film is synchronized to the ground speed of the aircraft so that the image being photographed remains fixed on the moving film. Advantages of strip photography include inherent continuous image motion compensation and, since it has no shutter mechanism, camera simplicity. Disadvantages include the need for accurate control of the film speed and poor high altitude performance. Strip cameras have been primarily used for low altitude, high speed reconnaissance applications. Since strip photography is well suited for linear study areas, it has been used extensively in commercial applications such as highway and railroad studies and selection of right of way for pipelines and power lines [9].

3.2 Linear TDI Arrays

The basic construction of a linear time-delay-and-integrate (TDI) array is shown in Figure 7. These arrays can be constructed from either CCD or CID unit cells. Such arrays come in various sizes such as 1024 by 64 element arrays with integration steps at 1, 4, 8, 16, 32, and 64 integrations. These arrays are operated in a mode analogous to a strip camera. The relative motion between the aircraft and the ground causes the image to move down the array from line to line. As the image moves, the charge analog of the image is electronically

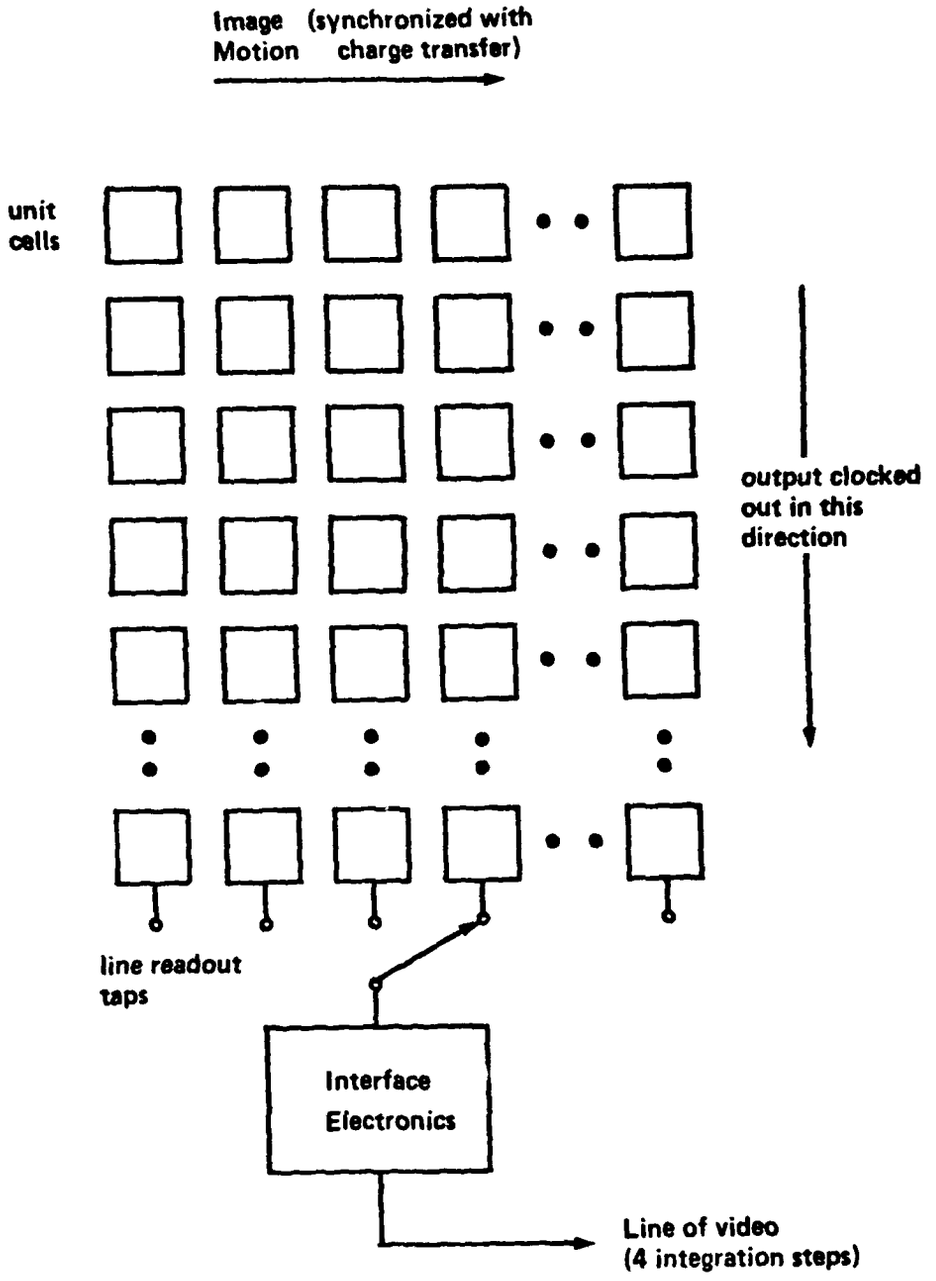

Figure 7. Linear TDI array.

shifted from line to line. Thus when the image reaches the last line of detectors, the charge for each point has been accumulated by several detectors. This integration of charge increases the sensitivity of the imaging device. Note that moving the charge analog of the image is analogous to moving the film in a strip camera. In the strip camera, the exposure is controlled by varying the width of the slit. In the TDI array, the exposure is controlled by reading out the signal at different lines or integration steps. That is, reading out the image at the eighth line would yield a signal which has accumulated charge for a shorter period of time than reading out a signal at the 32nd line. Therefore, the brighter the scene, the fewer number of lines are needed for integration. The number of integrations is constrained by the size of the array and also by the amount of charge a unit cell can store. "Overfilling" a unit cell can cause blooming of an image.

The output of a TDI array is therefore successive lines of the scene. It is then necessary to assemble these lines into a continuous picture. This procedure is complicated by the fact that the aircraft is moving and since each strip is taken at a different time, simply forming a photograph by assembling many lines would not be satisfactory for precise applications such as mapping. However, if the flight dynamics for each strip are known, a computer can process the strip data and assemble them into frame photographs. Thus it is possible that data from strip photography can be made useful on comparators designed to process frame photographs.

3.3 Processing of Strip Photography Data

Since a continuous strip photograph is usually not what is desired for various applications, a procedure for processing strip photography data into other forms such as frame photographs is needed. Furthermore, flight path nonuniformities such as roll, pitch, yaw, altitude, and speed cause distortions along the strip photograph which must be corrected.

In order to provide a means for performing computational operations for strip photography, mathematical procedures have been developed [9-13]. Case [11] suggested the use of Instantaneous Equivalent Frame Photos (IEFP) whereby all measured points are transferred from the strip to a ficticious frame photograph having the same focal length but a single instantaneous position and attitude. The selection of the position and attitude are chosen to minimize the deteriorating effects of constantly changing position and attitude. Derenyi's [11] method of line-to-line orientation is a similar concept. In this method the strips are projected down to the ground. After the measured strip coordinates have been projected, the resulting ground points are projected back up to the IEFP. Thus conventional frame photographs are constructed from many strip photographs with appropriate corrections applied.

Three analytic systems were proposed by Derenyi for the relative orientation of continuous-strip imageries produced by stereo systems [13]. The methods he described are applicable to continuous strip

cameras, side looking radars, and infrared line-scanner systems. The first of these proposed methods is a line-to-line orientation in which two lines of corresponding points are oriented relatively. In the second method small sections, rather than individual lines, are oriented relatively. Of course, it must be assumed that any changes which occur in the orientation of elements within these sections are negligible. The third method is a triple-channel recording scheme which uses a third channel providing a vertical view of the terrain in addition to the two regular stereo channels. This method is superior to the first two, however, it requires a more complicated sensor.

3.3.1 Line-to-Line Orientation

In a strip camera, all points in a single line are recorded simultaneously and thus have the same exterior orientation. It is therefore theoretically possible to orient two lines of corresponding points relatively regardless of any disturbing effects resulting from continuously changing orientation elements. Typically, the coplanarity condition is applied to carry out the relative orientation. Referring to Figure 8, the points on line BL have the same orientation elements as the points on AR. Thus subsequent line pairs can be oriented to previous ones and therefore changes in orientation elements at regular intervals along the strip can be determined.

There are, however, limitations to the line-to-line method. Since neighboring line models have no common points, transfer of the scale from line-to-line along the flight path is not possible. Also only

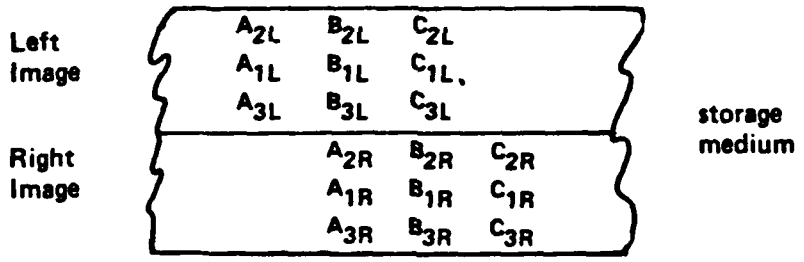

Figure 8. Storage of line data for line-to-line orientation [13].

three of the five independent orientation points can be found since the orientation points form a line rather than a plane. The other two must either be known or assumed to be zero.

Another limitation results from the fact that the look angle of the terrain points across the flight path is fixed. Therefore, terrain points which have different elevations are seen at different times. Thus, even if all points on the left image are recorded at the same instant, the recording of their corresponding points on the right image could be spread over an interval of time. One result of this is that the orientation parameters for the points in question in the right image could be nonuniform. Another negative result is that the base length from point pair to point pair is a function of the above mentioned time interval.

3.3.2 Section-to-Section Orientation

In this method it is assumed that changes which occur in the orientation elements within a section of the strip are negligible. Therefore, rather than taking a line as a unit, a small section of the strip is taken as a unit as shown in Figure 9. This method is similar to the line-to-line method.

The main limitation of the section-to-section method is that the orientation of a sensor does not actually remain constant, as was assumed, during the recording of a section. Derenyi [13] conducted a comprehensive study of the effect of the neglected changes in the

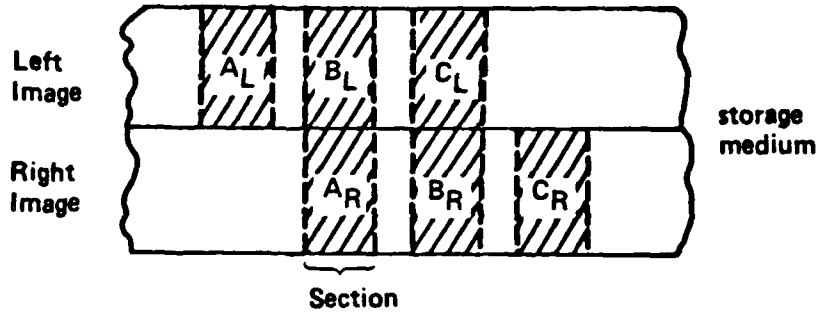

Figure 9a. Storage of section data for section-to-section orientation (13).

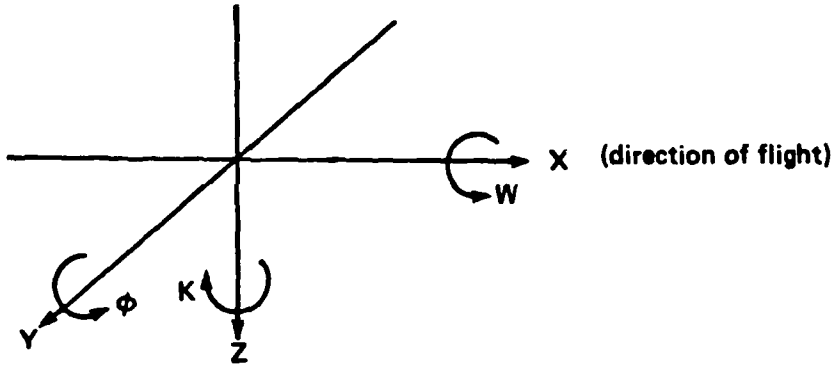

Figure 9b. Coordinate system.

orientation on the solution. The direction of flight is X, the transverse coordinate is Y, and the altitude is Z. Let ω, ϕ , and κ be the rotation about the X, Y, and Z axes respectively as shown in Figure 9b. It was found that small changes in dbz and dby can distort the solution of $d\phi$ and $d\kappa$. These are the two most critical elements. The solution for $d\omega$, dby, and dbz were approximately their average within a particular section. Lastly, it was found that the effect of nonuniformity of the orientation is inversely proportional to the length of a section. A longer section, however, weakens the validity of the constant orientation assumption since the recording time of the section is longer.

3.3.3 Triple Channel Recording

Derenyi suggested adding a third channel which views the terrain vertically downward. Thus the three channels will be forward, vertical, and aft. All three images would be recorded side by side as shown in Figure 10. Points which are recorded simultaneously by the three channels are equivalent to three lines on a frame photograph. Lines A , B , and C are equivalent to three lines on a frame photograph taken from the same space position. Lines A and C correspond to similar lines along the left and right edges of a frame photograph, and line B corresponds to a line passing through the principal point. With this scheme, a complete relative orientation, strip triangulation, and transfer of scale along the flight path are possible. Of course, considerable complexity is added to the sensor.

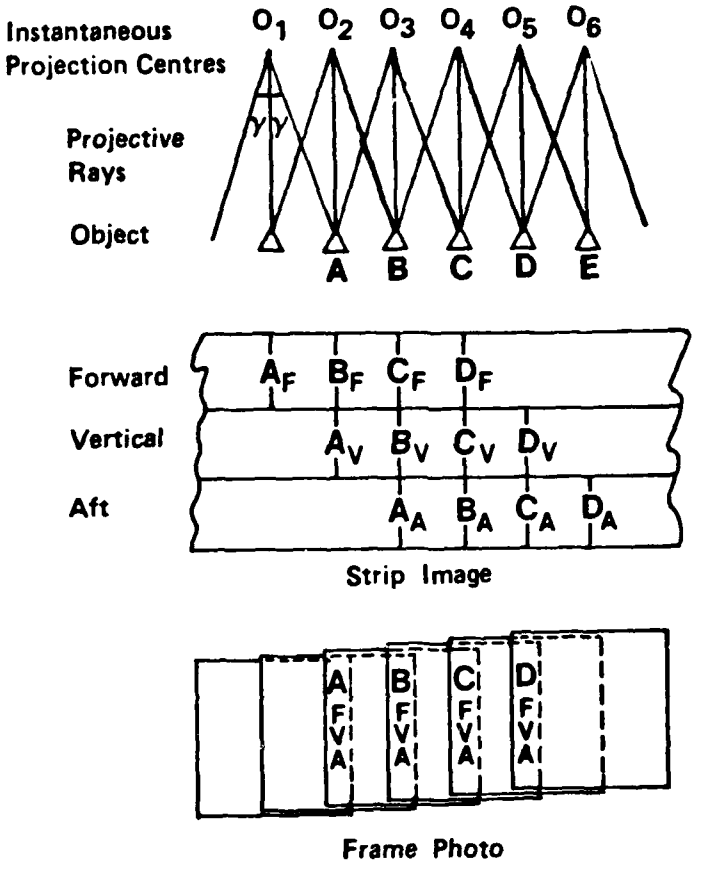

Figure 10. Storage of data for triple channel recording [13].

3.3.4 Processing Stereo Line Image Data

Recent work has been performed by Gibson [14] at the Canada Centre for Remote Sensing applying the procedures described above. The objective of this work is to establish the feasibility of using line scanning image sensors to produce imagery suitable for map making. The line imaging sensors used were visible/near infrared devices, however, the results are applicable to line scanning image sensors in general.

Gibson has recently studied two modes of stereo imagery. The first one used a Daedalus Multi-Spectral Scanner (MSS) which acquired data by flying parallel paths with 60% sidelap of the lines. The other set of data was obtained using the CCRS Multi-Element-Imaging-System (MEIS) II line imager. Two externally mounted mirrors provided both forward-looking and aft-looking channels. A third channel looking straight down was also used allowing the triple channel method described earlier to be investigated. An inertial navigation system (INS) was used to simultaneously record the flight dynamics of the aircraft. For the MSS data, a high altitude laser profiler was used to accurately record the altitude of the aircraft.

The data studied in this project was obtained from a five minute flight line at 8200 meters above ground level. The flight data which was analyzed consisted of pitch, heading, altitude, and velocity. Roll data was not used since both imaging systems had roll correction capability.

The imaging system had an instantaneous field of view per pixel of .7 milliradians resulting in a pixel size of 5.7 meters. The following is a summary of the pixel displacements resulting from aircraft motion on a typical mission [14].

Pitch angle variations had two observed components. One, resulting from the autopilot, was of large amplitude and low frequency. The other was a small amplitude, high frequency vibration induced component. The pixel displacements resulting from pitch angle displacements ranged from 1.3 to 16.2 pixels with a maximum change over a 20 second interval of 10.0 pixels.

Heading angle variations also were composed of both high and low frequency components. The effects of heading angle variations were calculated in terms of the relative shift of one end of the line with respect to the other. The pixel displacements ranged from 1.8 to 23.2 pixels with a maximum change in 20 seconds of 14.3 pixels.

Altitude changes caused a low frequency effect which highly correlates with pitch angle changes. The result of altitude changes is the apparent stretching or shrinking of the line of imagery on the ground. The resulting pixel displacement had a maximum of 5.1 pixels and a maximum change in 20 seconds of 1.1 pixels.

Velocity changes occur both along and across the flight track. Along track variations cause stretching or shrinking of the spacing of the image lines on the ground. The maximum pixel displacement caused by along track velocity variations was 13.1 pixels. Across track

variations cause a side or transverse shift of a line of imagery with respect to its nearest neighbors. The maximum pixel displacement resulting from this was 5.0 pixels. As can be seen from these data, very accurate flight dynamics data are needed to produce mapping quality images.

In processing the stereo line imager data, Gibson used techniques similar to those employed for conventional photography. That is, relative and absolute orientation parameters were obtained, however, the processing was complicated somewhat because of the need to remove low frequency errors of the inertial navigation system data. The coplanarity condition was used to relate the stereo images using ground points whose co-ordinates were not known. The collinearity condition was used for relating the imagery to known ground control points. Both the coplanarity and collinearity equations were linearized using the first term of a Taylor Series expansion. The resulting set of equations was used to calculate the short term offset and drift errors of the inertial navigation system data. Position and altitude data were then used for the geometric correction of the imagery data. The details of the coplanarity and collinearity condition equations and the geometric correction process can be found in a previous publication by Gibson [15].

In order to be able to compute run times, the number of operations per pixel and the number of operations per second of the computer must be known. Gibson, for example, used 1024 pixels per line and to

accomplish the necessary corrections to the raw data approximately 75,000 operations per line were required. Modern minicomputers are capable of 1 to 5 million floating point operations (MFLOPS) per second. These computers, therefore, would require approximately 15 to 75 milliseconds of computational time to process each line of the image. With modern microprocessors and optimized algorithms, a dedicated machine operating at 5 to 10 MFLOPS should be attainable. If custom Very-High-Speed-Integrated-Circuit (VHSIC) technology is used, speeds of up to 100 MFLOPS could be realized. Thus execution times of approximately 750 microseconds per line are theoretically possible. With such a dedicated processor, a 1024 line image could be processed in less than a second.

Note, however, these run time estimates are for processing the raw data and applying corrections for flight perturbations. Run time estimates for operations such as image translation, rotation, magnification, etc., are discussed in the Appendix.

4.0 Resolution Model

In the past, several methods have been proposed for the evaluation of swept linear array system performance. Trade-offs between resolution and detector signal to noise ratio (SNR) have determined optimal detector size as a function of optical modulation transfer function (MTF), detector physical characteristics, aperture, and contrast [16]. The effects of detector shape (rectangular or elliptical) and detector integration interval on system performance have also been modeled [17]. Angular uncertainty in swept linear detector arrays has been estimated for specific point tracking and aerial reconnaissance systems [18-20]. In most cases, these models apply only to specific applications because of simplifying assumptions made about detector geometry, blur circle, and other system parameters.

The system resolution model described in this section assumes fewer design constraints. Recognizing the conflicting requirements of high spatial resolution (small detector elements) and high signal-to-noise ratio (large detector area), the object of this analysis approach is to quantify the trade-offs between optical performance, platform vibration, flight dynamics, resolution, and detector geometry for a swept linear array imaging system. The scenario shown in Figure 11 assumes a linear time-delay-and-integrate (TDI) array used in a push-broom scan mode. This model, however, is general enough to accommodate staring arrays or mechanically swept linear arrays with interleaved detector elements.

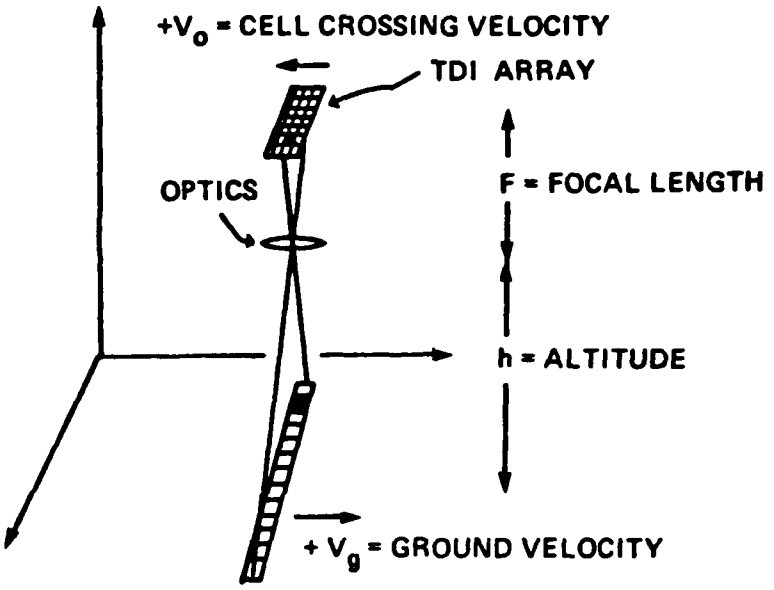

Figure 11. Push-Broom Scanned Array.

4.1 Resolution of Solid State Imagers

Traditional sampling theory assumes an ideal spatial (two dimensional) sampling function

$$s(x,y) = \sum_{i=-\infty}^{\infty} \sum_{j=-\infty}^{\infty} \delta(x-i\Delta x, y-j\Delta y) \qquad (1)$$

that is composed of an infinite array of Dirac delta functions [21]. Given a spatially bandlimited image, the sampling period must be equal to or greater than one-half the period of the finest detail (or spatial frequency) in the image if it is desired to reconstruct a sampled image having the same detail. This is, of course, equivalent to the well known sampling theorem of Shannon. The spacing of Dirac delta functions is given by the Nyquist criterion

$$\Delta x \leq \frac{2\pi}{w_x} \qquad \Delta y \leq \frac{2\pi}{w_y} \qquad (2)$$

where w_x, w_y are image cutoff frequencies. The importance of two-dimensional sampling theory is that it sets a theoretical limit on the spatial frequencies that may be reconstructed from sampled images.

Practical imaging focal plane arrays or linear scanned arrays cannot achieve the performance of ideal sampling functions. The consequence of using sampling pulses of finite width instead of Dirac delta functions is that the image may be undersampled. Since the signal-to-noise ratio of a detector element is related to the amount of

incident quantum energy integrated in time and space, designers try to maximize the detector responsive area.

Staggered arrays and TDI arrays are two approaches used to maximize detector area under a centerline spacing constraint. The ratio of detector centerline spacing to detector width is called the fill factor. Fill-factors less than unity may be due to geometric design constraints. Fill-factors greater than unity are possible in linear scanned arrays having even and odd detectors in two staggered rows as shown in Figure 12.

Practical imaging systems not only sample with finite width pulses, but they sample moving images over some finite time period. Image motion relative to the focal plane causes a blurring effect. This effect contributes to reduced resolution of the reconstructed image in addition to sampling pulse (spatial) effects. Image motion might result from motion of the image itself (moving tanks,ships), from vibration of the sensor platform (reconnaissance aircraft), and from the mechanical scanning of the detector element or array. Cell crossing velocity refers to the velocity of a blur spot of a point source as it crosses a detector element.

Optical system designers often use an arbitrary but useful measure of resolution, the Sparrow criterion, as an indication of limiting performance for a given size system [22]. According to this criterion, two adjacent point sources (not necessarily of equal intensity) are considered resolved if their combined diffraction pattern on the focal plane has no maximum between the two point-images.

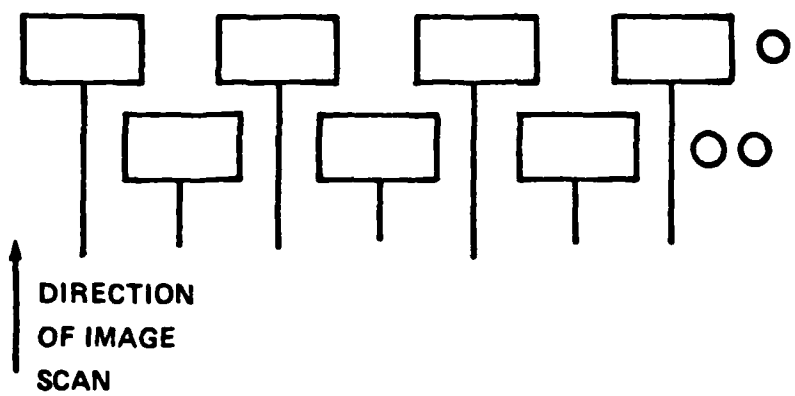

FIGURE 12. Linear Array with Staggered Detectors.

A definition of optimal resolution for solid-state imaging systems is presented in this section that combines the concepts of sampling theory and the Sparrow criterion. With such a model, a systems analysis can be performed to calculate the resolution of a given system. Such factors as detector geometry, optical components, electronic timing, and virtual image motion can be considered. The model is novel in that it combines specifications of the optical train, stabilized platform, detector array, flight dynamics, and electronics into one model.

By the Nyquist criterion, the smallest resolvable detail is given by

$$R \leq 2d \tag{3}$$

where d is the centerline spacing between detector elements. Depending on the width of the point spread function, resolution can be much worse than this but it can never be any better. A definition of resolution for two point sources on a detector array must be modified from a continuous Sparrow criterion since resolution must be an integer multiple of d. Let the discrete Sparrow criterion be defined such that two adjacent point sources are resolved if the energy of their combined sampled point spread functions do not have a unique maximum. Figure 13a illustrates the quantum energy from a single point spread function integrated by detector elements. Figure 13b and 13c show two sets of point spread functions spaced at a distance 2d apart. The sample period is d in both cases. In Figure 13b the two points are resolved. In Figure 13c, however,

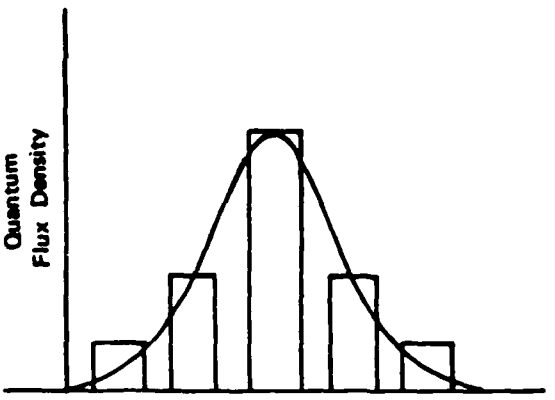

Figure 13a. Quantum energy integrated by detector elements from single point spread distribution.

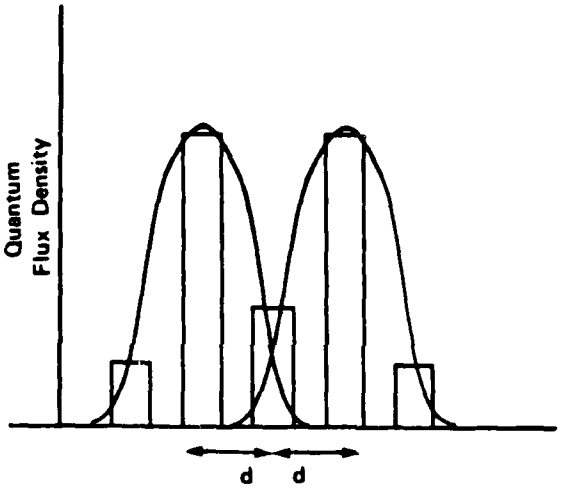

Figure 13b. Two points resolved at Nyguist rate.

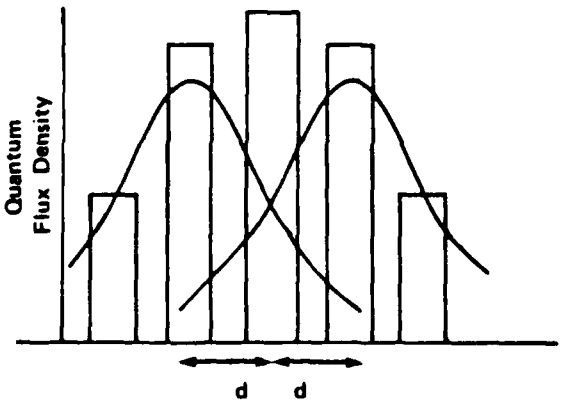

Figure 13c. Two points unresolved.

the energy of the combined sampled point spread function has a single maximum and thus the two points are not resolved.

The discrete Sparrow criterion may be expressed very simply if we consider only noiseless optimal resolution of two equal energy point sources. Assume a point spread distribution centered on a detector element, as shown in Figure 13a. Denote the quantum energy incident on that detector over some time interval as Qo. Let Q1, Q2, Qn represent the energy from the same point source falling on adjacent detector elements. Two equal energy point sources are resolved at a minimum distance of 2d on the focal plane if

$$Q_o > 2Q_1 - Q_2 \tag{4}$$

The point sources are assumed to be noiseless and contributions to Qi from other sources are neglected.

The decision to define resolution in terms of point sources is arbitrary. Though it is one of many ways to characterize system resolution, it facilitates the calculation of constraints necessary to achieve Nyquist sampling.

Resolution is not the same thing as radiometric accuracy. The resolution of a solid state sensor system is ultimately limited by the spatial sampling rate or detector spacing. However, sub-pixel accuracies are possible whenever correlation in time or space exists. Automated edge location measurements of images have achieved accuracies of better than 0.30 pixels in the presence of 10% RMS noise [23].

Greater accuracies have been demonstrated by applying Kalman filtering techniques to the tracking of moving point sources.

Using a resolution criteria based on point sources, a point spread function is derived which describes light intensity incident on the focal plane. The shape and width of a point spread function depends on optics, image motion (due to object or camera motion) and atmospheric effects. Careful optical design can minimize image degradation due to diffraction limiting and optical aberration effects.

Blur resulting from several sources is conservatively estimated by summing blurs resulting from individual aberrations and diffraction limiting effects [24]. Individual blur spot sizes may be estimated from lens type, focal length, and aperture. Platform vibration occuring during a charge integration period, has the multiplicative effect of spreading the blur. Assuming, as does [20], that the resulting point spread function is Gaussian distributed, the Gaussian shaped profiles are easily convolved.

$$B = 2\delta_{image} = 2(\delta^2_{lens} + \delta^2_{vibration})^{1/2} \tag{5}$$

The resulting measure of image blur is easily translated into a point spread function.

$$S(x) = \frac{1}{\sqrt{2\pi\delta^2}} \cdot \exp \frac{-x^2}{2\delta^2} \tag{6}$$

Generation of the point spread function from optical and vibration parameters is shown schematically in Figure 14.

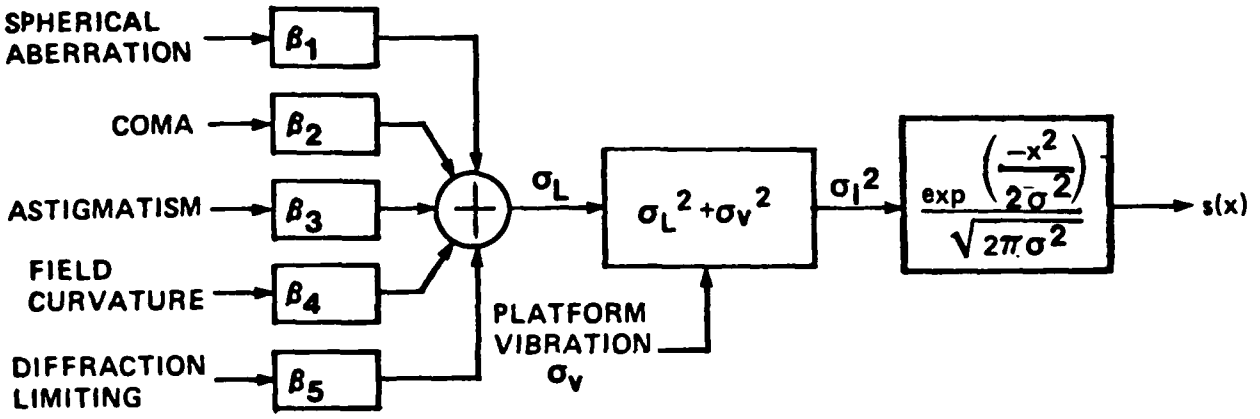

Figure 14. Point Spread Function Model.

4.2 System Model

An aerial reconnaissance scenario, illustrated in Figure 11, assumes a linear time-delay-and-integrate (TDI) array used in a pushbroom scan mode. This model, however, is general enough to simulate staring arrays, as well as mechanically scanned linear arrays with interleaved (fill factor greater than unity) detector elements.

Whereas point spread functions depend on optical performance and platform vibration, system resolution depends on three additional parameters: flight dynamics, detector geometry, and TDI timing. The quantum charge accumulated under each detector element is determined by integrating the moving point spread function with respect to these three parameters. It is possible to determine conditions which maximize detector responsive area for a Nyquist sampling rate by applying the Discrete Sparrow Criterion to the discrete integrated charge function.

As can be seen in Figure 11, flight dynamics affect the cell crossing velocity or, equivalently, the velocity which a point spread function moves across a detector cell or element. Since level, straight, and constant velocity flight is assumed in this simulation, cell crossing velocity is

$$V_c = \frac{V_g \cdot f}{h} \tag{7}$$

where Vg is the sensor velocity with respect to ground, h is the altitude of the sensor and f is the focal length of the sensor optics.

Detector centerline spacing, d, and fill-factor are two detector geometry parameters modeled in this simulation. As previously discussed, a smaller fill-factor move closely approximates a Dirac delta function at the cost of detector signal-to-noise ratio.

A unique function of this model is that the TDI charge integration period, τ_I , is not necessarily equal to τ , the time required for a blur spot to travel from one detector element to another. In this model it is assumed that

$$\tau \geq \tau_I \tag{8}$$

In other words it is not assumed that a detector is always "on" and thus accumulating signal. Consider, for example, a CID element which is turned "off". During the time the element is off, charge carriers which are generated by incident radiation are not accumulated but are injected into the substrate and lost. This model has the flexibility to handle such a situation.

Radiant energy originating from a point source and incident on a detector element is found by integrating flux density, described by a point spread function S(x), incident at the detector during one integration period. Quantum flux (for a one-dimensional case) is given by

$$\phi_e(x) = \int_{x-w/2}^{x+w/2} S(x)dx \tag{9}$$

where S(x) is a Gaussian point spread function. Assuming a constant

ground velocity, we have

$$\phi_e(t) = v_c \int_{v_c t - \frac{w}{2}}^{v_c t + \frac{w}{2}} S(v_c t)dt \qquad (10)$$

Integrating (10) over one integration period results in the incident energy on the i-th detector elements.

$$Q_i(\tau_I) = \int_{t_o}^{t_i} \phi_e(t)dt \qquad (11)$$

where

$$\tau_I = t_i - t_o \qquad (12)$$

Combining (11) and (12) and solving for an equality results in a limit for the system parameters meeting the optimal resolution criteria.

4.3 Application of the System Model

The resolution model presented in this section provides a framework for the analysis of imaging systems using discrete arrays. This model can be applied for systems employing staring array sensors as well as electronically or mechanically scanned linear arrays. By varying system parameters, it is possible to determine the best trade-offs between these system parameters and system performance. System parameters included in the resolution model fall into three categories. These are optical system parameters, focal plane parameters, and flight dynamics parameters.

The optical system parameters include aperture size, focal length, abberations, astigmatism, and other influences on the point spread function. These are constrained for the most part by the state-of-the-art in optical lens manufacture.

The sensor or focal plane parameters include detector geometries, fill factors, TDI charge integration period, and centerline spacing. The system designer must determine the optical trade-offs with respect to these parameters while keeping in mind the importance of considering noise sources.

Flight dynamics parameters include sensor velocity, altitude, and platform vibration. These parameters are constrained largely by the available airborne platform and the particular mission scenario.

By modeling a system using the resolution model, one must assume certain parameter values consistent with the mission scenario and system specifications. By varying the values of focal plane parameters, it is possible to determine the best system trade-offs and optical parameter values.

5.0 Conclusions and Recommendations

A survey of existing IR imaging systems has been performed. The most promising systems for use for aerial photography are scanned linear arrays of CCD or CID unit cells operated in a time-delay-and-integrate (TDI) mode. These types of imaging systems are basically an electronic strip camera. Imagery produced by these systems, after suitable data processing, can be used for mapping and targeting applications. Gibson reported maximum pixel displacements during a 20 second interval for uncorrected imagery to be 10.0 pixels for pitch angle variations, 14.3 pixels for heading angle variations, 1.1 pixels for altitude changes, and 5.0 pixels for velocity changes. From these data it is obvious that uncorrected imagery is not accurate enough for most mapping and targeting applications. When high accuracy is required, three dimensional flight data such as that from an inertial navigation system, should be simultaneously recorded with the imagery. It is theoretically possible to perform corrections on existing imagery using known ground points rather than flight data. Such a process, however, is tedious and dependent upon the imagery itself. Correction of such imagery, therefore, is not amenable to developing generalized software and would be limited to very special applications.

A system model useful for calculating the resolution of an imaging system was also developed. This model, which is adaptable to linear swept arrays as well as two-dimensional staring arrays, can be used to calculate or to perform system design trade-offs under a system resolution constraint.

It is recommended that future systems go to an all digital format in order to capitalize on the advances in computer image processing and computer graphics. Such systems could store both visible and IR imagery in the same format allowing the use of the same computer processing. Both visible and IR imagery could be recorded simultaneously along with the flight data. After processing it would then be possible to electronically display either or overlay both images. Other advantages of an all electronic digital system include the increased dynamic range of electronic systems over film, the elimination of expensive and restrictive mechanical systems for plotting and display, accurate and fast x and y coordinate computation since each pixel is digitally stored, the elimination of film induced distortions, and the ability to scroll through a flight path on a CRT essentially as though you were looking down from the aircraft [14,15].

Appendix - Real Time Response

A requirement exists for an analytical stereoplotter featuring the realtime response of digital stereomodels to handwheel and footwheel movements. In order to establish the feasibility and design of such a system, a definition of "real-time" is needed. The following section defines the term in the context of this project, recommends a computer response time, and discusses the trade-offs in the design of such a real-time system.

In a real-time digital analytical stereoplotter (DAS) or stereocomparator, there should be no perceptible time lag between the handwheel and footwheel movements and the movement of the floating mark. To meet this requirement, the response time of the image processing hardware should be less than the human response time visual stimulus. Since real-time DAS response places such great demands on the image processing equipment, a trade-off exists between what is an acceptable DAS response time and hardware complexity, cost and risk (feasibility).

Reaction time varies among humans as well as with the sensor used [25]. The quickest reaction time is in response to a sound and is about 150 milliseconds. Response to a tactile sensation of pain may take up to 700 milliseconds. Under ideal circumstances, a "fast" person can react to a visual stimulus in 200 milliseconds. This does not imply that a computer response time of 190 milliseconds will go unnoticed, but that it will result in a combined system response time

of 390 milliseconds.

Computer ergonomic studies have provided recommendations for maximum acceptable computer response time for various tasks [25-27]. The recommended response time measured from the act of drawing with a light pen to a visual response was 100 milliseconds. Longer response times resulted in a noticeable lag and loss in productivity. The same response time was reported for acoustic feedback, such as a "click", in response to a key depression.

Manipulating computer imagery in real time can be a difficult and computation intensive operation. As a simple example, consider an image of 512 pixels per line by 512 pixels per line with eight bits per pixel. This corresponds to a moderately high resolution video image. The generalized linear transformation or affine transformation represents axonometric distortions where parallel straight lines map into parallel straight lines. This algorithm is given by:

$$p = a_o + a_1 j + a_2 k \qquad \text{(A1)}$$

$$q = b_o + b_1 j + b_2 k \qquad \text{(A2)}$$

where (p,q) represent the transformed pixel coordinates and (j,k) represent the original pixel coordinates. The affine transform is used for image translation, rotation, and scale change. To generate a new set of coordinates for each pixel in this example requires 1,048,576 additions and 1,048,576 multiplications. Since the new coordinates may not fit the grid format of the video raster display, a resampling function is necessary to assign values to all new pixel locations. The

simplest and least accurate resampling function is the nearest neighbor algorithm. In this algorithm, a pixel location assumes the value of the transformed pixel closest to it. This algorithm is not accurate enough for most applications, least of all for mapping applications. Assuming that it is equivalent to the affine transform and that the video frame memory is updated every 100 milliseconds, over 20 million additions and floating point multiplications will be required every second. More stringent requirements to increase resolution and or more precise resampling can easily increase the data processing burden by several orders of magnitude.

LIST OF REFERENCES

1. Chan, William S., "Focal Plane Architecture: an Overview," Optical Engineering, Vol. 20, pp. 574-578, Jul/Aug. 1981.

2. Chan, William S., Editor, Proceedings of the S.P.I.E., "Mosaic Focal Plane Technologies," S.P.I.E., Bellingham, Wa., 1980.

3. Chan, William S., Editor, Proceedings of the S.P.I.E., "Advances in Focal Plane Technology," S.P.I.E., Bellingham, Wa., 1980.

4. Michon, G.J. and Burke, H.K., "Charge Coupled Devices," Topics in Applied Physics, Springer-Verlay, Berlin, 1980.

5. Krikorian, Esther, Editor, Proceedings of the S.P.I.E., "Infrared Image Sensor Technology," S.P.I.E., Bellingham, Wa., 1980.

6. Spiro, Irving J., Editor, Proceedings of the S.P.I.E., "Utilization of Infrared Detectors," S.P.I.E., Bellingham, Wa., 1980.

7. Electronics Division of the I.E.E., International Conference on Advanced Infrared Detectors and Systems, Bamber Press LTD, London, England,1981.

8. Wight, Ralph, "Sensor Implications of High Altitude Low Contrast Imaging," Photogrammetric Engineering and Remote Sensing, Vol. 45, pp. 63-66, Jan. 1979.

9. Ghosh, Sanjib K., Analytical Photogrammetry, Pergamon Press, New York, 1979.

10. D. G. Elms, "Mapping with a Strip Camera," Photogrammetric Engineering, Vol. 28, No. 4, pp. 638-653, 1962.

11. J. B. Case, "The Analytical Reduction of Panoramic and Strip Photography," Photogrammetria, Vol. 22, No. 4, pp. 127-141, 1967.

12. S. E. Masry, "Analytical Treatment of Stereo Strip Photos," Photogrammetric Engineering, Vol. 35, No. 12, Dec. 1969, pp. 1255-62.

13. E. E. Derenyi, "Orientation of Continuous Strip Imagery," Photogrammetric Engineering, Vol. 39, No. 12, pp. 1329-35, Dec. 1973.

14. J. R. Gibson, "Processing Stereo Imagery from Line Imagers," Presented at the International Geoscience and Remote Sensing Symposium, Aug. 27-30, 1984, Strasbourg, France.

15. J. R. Gibson, et.al., "A Stereo Electro-Optical Line Imager for Automated Mapping," Proceedings of the Sixth International Symposium on Automated Cartography.

16. W. C. Bradley, "Small Geometry Charge Coupled Devices for Aerial Imagery," Airborne Reconnaissance III, Proc. SPIE, Vol. 137, pp. 116-120, 1978.

17. D. E. Marshal, Jr., "Focal Plane Array Design for Optimal System Performance," Infrared Imaging Systems Technology, Proc. SPIE, Vol. 226, pp. 66-73, 1980.

18. V. V. Vaughn, E. L. Bosworth, and D. D. Dudley, "Angular Measurement Uncertainty for an Infrared (IR) Sensor," Infrared Systems, Proc. SPIE, Vol. 256, pp. 68-73, 1980.

19. R. Lyon, R. E. Othmer, and I. W. Doyle, "Computerized Performance Predictions for a Solid State Reconnaissance Camera," Aerial Reconnaissance Systems, Proc. SPIE, Vol. 79, pp. 217-227, 1976.

20. S. A. Hempenius, "The Role of nage Quality in Photogrammetric Pointing Accuracy," Final Repoit to European Research Officer, U. S. Army, Contract No. DA-91-591-EUC-3721.

21. W. K. Pratt, Digital Signal Processing, John Wiley, New York, pp. 93-99, 1978.

22. W. L. Wolfe, G. J. Zizsis, The Infrared Handbook, Ofice of Naval Research, Wash. D. C., 1978.

23. J. D. Thurgood, E. M. Mikhail, "Photogrammetric Aspects of Digital Images," Proc. ACSM-ASP, pp. 295-304, 1982.

24. R. Welch, "Progress in the Specification and Analysis of Image Quality," Photogrammetric Engineering and Remote Sensing, Vol. 43, No. 6, pp. 709-719, June 1977.

25. Robert W. Bailey, Human Performance Engineering, Prentice-Hall, Englewood Cliffs, N.J., 1982.

26. R. B. Miller, "Response time in man-computer conversation transactions,"
AFIPS Conference Proceedings (Fall Joint Computer Conference, 1968) Washington, D.C., Thompson Book Co., 1968.

27. S. E. Engel and R. E. Granda, "Guidelines for man/display interfaces," IBM Technical Report, TR00.2720. Poughkeepsie Laboratory, Dec. 1975.

MISSION
of
Rome Air Development Center

RADC plans and executes research, development, test and selected acquisition programs in support of Command, Control, Communications and Intelligence (C^3I) activities. Technical and engineering support within areas of competence is provided to ESD Program Offices (POs) and other ESD elements to perform effective acquisition of C^3I systems. The areas of technical competence include communications, command and control, battle management, information processing, surveillance sensors, intelligence data collection and handling, solid state sciences, electromagnetics, and propagation, and electronic, maintainability, and compatibility.

END

DTIC

7-86